Annals of the Academy of Romanian Scientists
Edition ONLINE Physics Series
ISSN 2066-8589 Volume **1**, Number **2**/**2009**

MICROSTRUCTURAL CHANGES IN OXIDIZED Zr-2.5%Nb ALLOY BY THERMAL TRANSIENTS

M. MIHALACHE [1], V. RADU[2], T. MELEG[3], M. PAVELESCU[4]

Abstract. *The experimental simulation of LOCA scenarios in CANDU reactors assumes transients of temperature on the pressure tubes from fuel channels. In case of a postulated accident of this kind, which is supposed to occur after some hot years in normal operating conditions, the safety analysis should take into account the oxidised state of pressure tube and the changes of its microstructure during the ramps temperature as well. This paper investigates the micro-structural changes in oxide layers and material base (Zr-2.5%Nb) resulted from specific thermal transients. This study was realised on Zr-2.5%Nb alloy samples, which were previously isothermally oxidized at temperature of 700^{o}C for different time intervals. Afterwards, the resulted samples with variables thickness oxide layers were subjected to the various temperature transients at different heating/cooling rates. The oxidation process in steam was carried out in a thermobalance facility. Using the thermo gravimetric analysis (TGA) module it is possible to make in-situ measurements of weight gain. The isothermal oxidized samples were heated and cooled in thermobalance furnace at different controlled rates. Subsequently, the oxidized Zr-2.5%Nb samples were investigated by: optical microscopy, scanning electron microscopy (SEM) and EDS (energy dispersive X-ray spectrometry). The paper presents some results of experimental investigations, mainly focused on the oxide layers and changes of alloy microstructures*.

Keywords: oxidation, oxide, Zr-2.5%Nb samples, X-ray spectrometry, oxide layers, alloy microstructures

1. Introduction

Pressurized Heavy Water Reactor (PHWR) uses zirconium base alloys due to their low neutron absorption cross-section, low irradiation creep and high corrosion resistance in operating reactor conditions. Zr-2.5%wtNb alloy, used for pressure tubes from fuel channels, has replaced Zircaloy-2 due to better physical and mechanical properties. The temperature of coolant fluid from pressure tubes inside varies from 260^o C (inlet) to 310^o C (outlet) and its pressure is in 9 to 11 MPa range. Manufacture processes suppose thermal treatments and a highly anisotropic hexagonal close packed (HCP) microstructure is obtained as fabricated.

In analysis of loss-of cooling accident (LOCA) the requirement is to maintain the integrity of pressure tube, a third barrier for gas fission products released. During

[1]Institute for Nuclear Research, Pitești, Romania (e-mail: mihalache.maria@nuclear.ro).
[2]Institute for Nuclear Research, Pitești, Romania.
[3]Institute for Nuclear Research, Pitești, Romania.
[4]Academy of Romanian Scientists, Bucharest, Romania.

LOCA, when pressure tube contacts the calandria tube, a heat transfer between cooling agent and moderator occurs, and it deteriorates if at pressure tube inside surface has grown an oxide layer or if this layer is produced during thermal transients. The thermal properties of oxide are expected to be different from those of alloy, the effect of an oxide layer being the restriction of heat flux transferred to moderator, and a delay of heat is released. The temperature distribution in pressure tube walls changes in the case of oxide absence. The changes of morphology of zirconium oxide like as layering, spalling, porosity increasing can alter the heat transfer by pressure tube wall.

One of major factors affecting the behaviour of tube and the possibility of its failure is the oxidation in steam at high temperature. The pressure tube may fail due to embrittlement by oxygen, and the formation of an oxide layer and the diffusion of oxygen into the sublayer metal can affect the strength and ductility of pressure tube and lead to failure.

The extent of problem is the accurate prediction of oxide response at thermal stresses produced by thermal transients specific at LOCA. Therefore, the behavior investigation in thermal transients of oxide layers have grown on the Zr-2.5%Nb alloy pressure tubes, similar to those from postulated accident conditions can provide a lot of information for the problem above described.

In addition, various methodologies applied for NPP safety and its management request the continuously improvement of materials database and models for accurate behavior of fuel channel components during accident scenarios.

In this report we study pressure tube oxidation and embrittlement, covering areas consisting in: isothermal oxidation and kinetics at 700ºC, changes of microstructure and behavior of oxidized alloy in thermal transients with different temperature increasing rates, elemental composition determining and measurement of oxygen profile in metal sublayer and in oxide. The main tools for evaluations is based on scanning electron microscopy (SEM) by processing of different signals such as secondary electrons, backscattered electrons and also based on energy dispersive X-Ray spectrometry (EDX) and characteristic X-ray spectrum processing.

2. Experimental procedure and material

In Institute for Nuclear Research have been performed recently thermal tests to investigate the embrittlement behaviour of Zr-2.5%Nb alloy during oxidation and the effect of pre-oxidation under LOCA conditions. The base material used in this study was cold worked Zr-2,5%Nb alloy from CANDU pressure tubes.

In these tests, few Zr-2.5%Nb cylindrical samples, having 10 mm length and a diameter of 4mm were employed. Using a thermobalance SETARAM SETSYS

EVOLUTION, the specimens were heated up to temperature of 700°C and were isothermally oxidised for different time intervals, in a flowing steam, in the furnace of thermobalance. The temperature gradient along the whole gauge length is kept at values less than 3°C. The temperature was measured by a Pt - PtRh10% thermocouple. In figure 1 is presented a functionally diagram of Setsys Evolution Thermoanalyser.

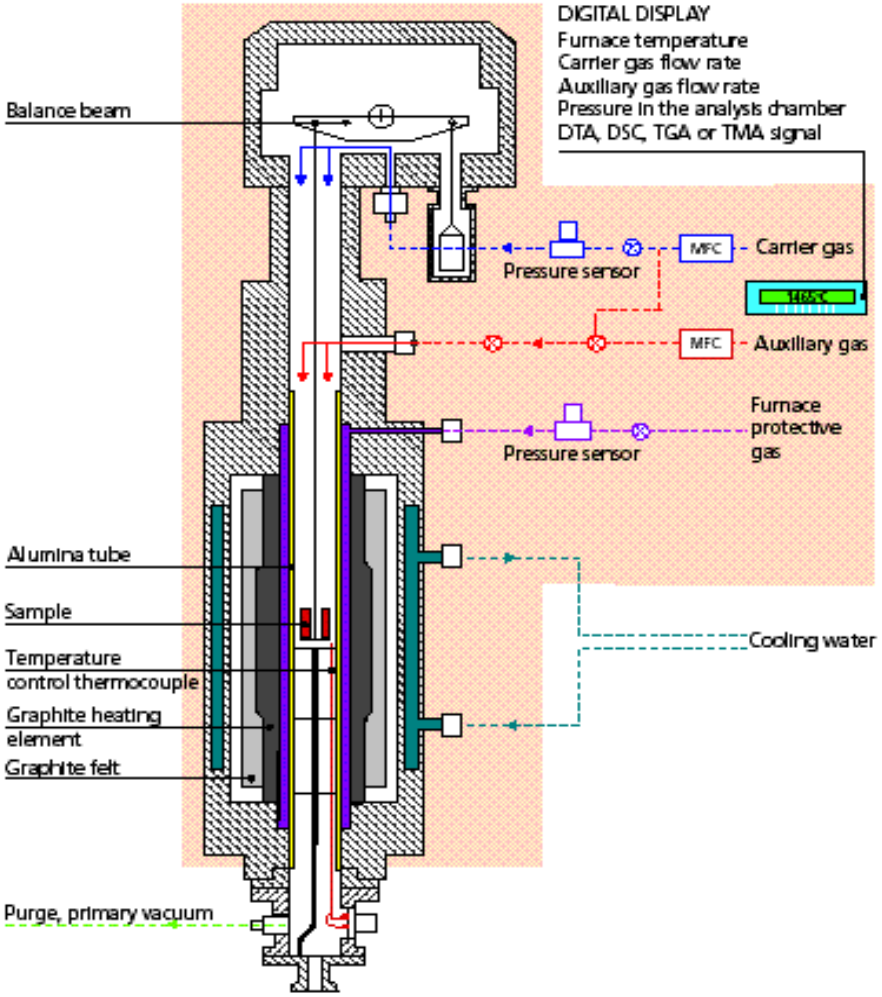

Fig. 1. Diagram of Setsys Evolution thermoanalyser.

The Wetsys controlled humidity generator ensured the humidity level control and regulation. The weight gain of the samples was measured in situ, the weight resolution of balance was 0.03 µg, the range of maximum measurable weight change is 400 mg, and the maximum sample weight is 20 g. For sample holder, a standard DTA rod was used and worked in TGA alone version (without connections for other signal acquisition).

In Table 1 are presented the parameters (T - temperature, S - surface, t - oxidation time, m_i, m_f – initial and final weight) and results of oxidation process (Co - oxygen concentration, t_{mas} - measured thickness) on the 3 samples.

After oxidation, to simulate LOCA conditions, the samples supported temperature increment and decrement in 600 – 1000^{o}C range of temperature with various rates: 3, 10, 30, 50, 75 ^{o}C/min. For examined samples, the order of transients is presented in table 2.

Table 1. Oxidation process parameters and results

Sample code	m_i **(g)**	T **(^{o}C)**	t **(h)**	m_f **(g)**	Δm **(mg)**	$\Delta m/S$ **(mg/dm^2)**	t_{mas} **(µm)**	C_{Ox} **(%wt.)**
P1	0.74449	700	3	0.74785	3.36	203.33	9	0.451
P2	0.77052	700	6	0.77512	4.60	276.03	10	0.597
P4	0.74200	700	1	0.74376	1.76	106.99	7	0.237
P7	0.72622	700	28	0.73485	8.63	531.57	25	1.188

where: T – temperature, S – surface, t – oxidation time, m_i, m_f – initial and final weight, C_{Ox} – oxygen concentration, t_{mas} – measured thickness.

We have to notice that zirconium oxide is a nonconductive material and its morphology is rather difficult to be examined by means of scanning electron microscopy.

Table 2. Order of thermal transients

Sample/order	**1**	**2**	**3**	**4**	**5**
P1	10 ^{o}C/min	30 ^{o}C/min	50 ^{o}C/min	3 ^{o}C/min	75 ^{o}C/min
P2	50 ^{o}C/min	3 ^{o}C/min	10 ^{o}C/min	30 ^{o}C/min	75 ^{o}C/min
P7	30 ^{o}C/min	3 ^{o}C/min	10 ^{o}C/min	50 ^{o}C/min	75 ^{o}C/min

3. Results and discussions

In figure 2 are displayed two in-situ measurements for weight gain in dependence on time, for sample P1, respectively P2).

The kinetic equation in case of P1-sample follows the relationship [1]:

$$\Delta w = 0.003 + 0.04269 t^{0.491} \quad (1)$$

The weight gain could be considered as a parabolic dependence on time variable (n = 1/2).

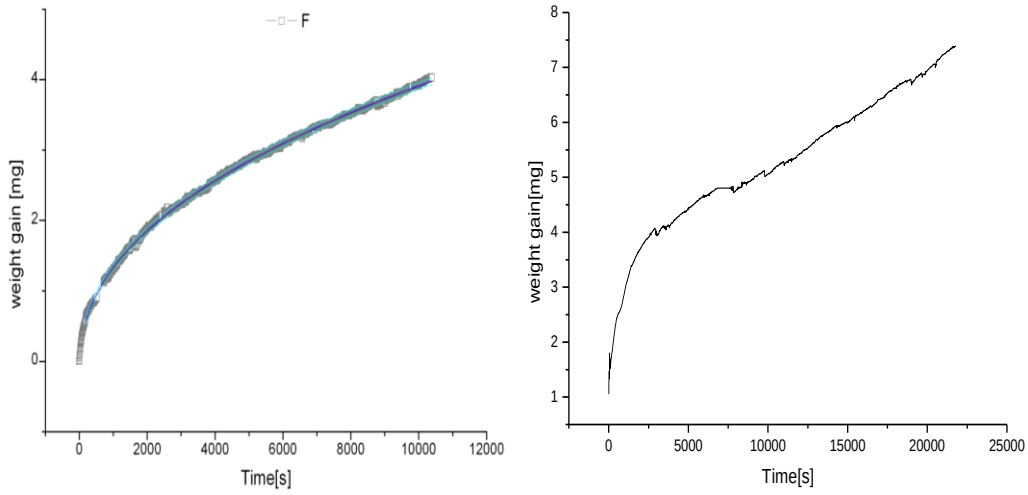

Fig. 2. Time dependence of weight gain (P1, respectively P2 sample).

For P2 sample, the plot is split into two functions: first one as a power function, and second one following a linear dependence. The kinetic equations are [1]:

$$\Delta w = 0.4854 + 0.228t^{0.345} \quad (2)$$

for t < 7500 s,

$$\Delta w = 3.25 + 0.00019\ t \quad (3)$$

for t > 7500 s.

The similar and distinctive features of samples could explain some differences in the oxidation kinetics.

Investigation of oxide surface morphology shows different aspects. The P1 sample, oxide surface (Figure 3a) presents crack planes growing in various directions; whereas the P2 sample surface (Figure 3b) displays spalling features. The last ones can be explained by the high accumulated stresses at metal-oxide interface which produce small pressured bubbles. This may be an effect of water vapour lack in the environment. In addition, the P2 sample surface exhibits a double oxide layer.

During pressure tube fabrication, the extrusion and cold-drawing processes results are turned up in a dual phase α/β structure with a defined texture. The α–phase grains have platelets form (containing 0.6 - 1% Nb in solution) with aspect ratios of 1, 10 and 40 in radial, transverse and longitudinal directions, respectively. The α grains are stacked together and separated by non-equilibrium β phase ~ 20%Nb. A cross-section down the axis of the tube exhibits a α/β structure typically uniform and elongated in transversal direction as in Figure 4.a).

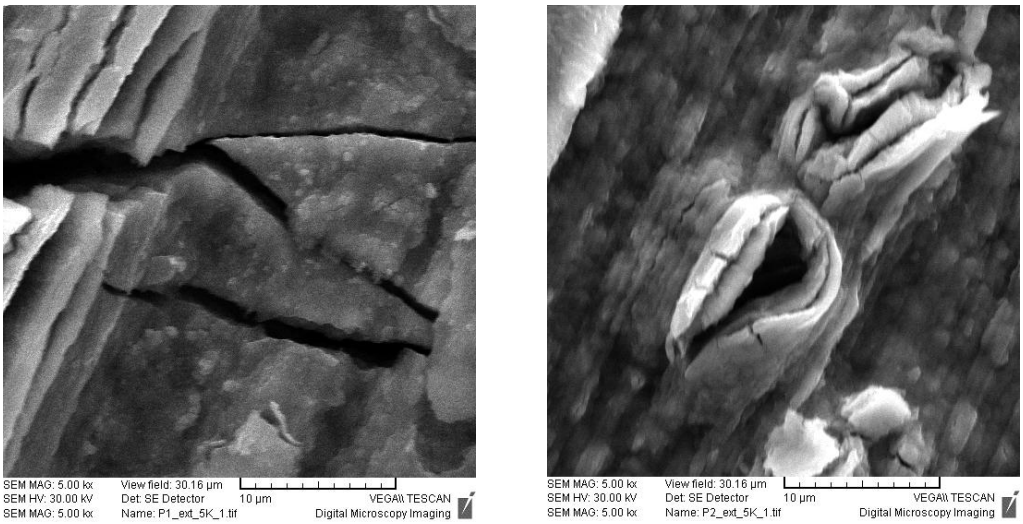

a) P1 (×5000) **b) P2(×5000)**

Fig. 3. Secondary electron images of oxide surface from **a) P1** and **b) P2** samples.

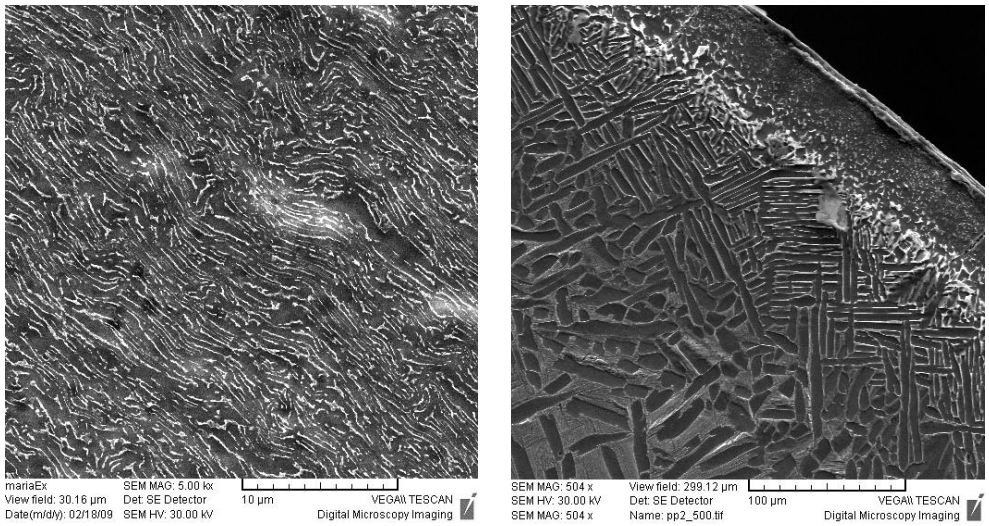

a) ×5000 **b) ×500**

Fig. 4. Secondary electron (SE) images of grains and texture in **a)** as received pressure tube **b)** in P2 sample.

The cross-section of the oxidised samples at high temperature (700 ^{o}C) displays a layered structure containing four regions of differing properties. Figure 4.b is an secondary electron image of grain morphology in P2 sample after thermal transients. It shows a resulting structure which contains:

- an oxide layer;

- a layer with equi-axed grains;
- a layer with Widmanstatten mixture of α/β plates (structure containing Widmanstatten features is known to have high corrosion and deuterium uptake rate in out-reactor tests);
- a specific layer with α grains which grew-up inside of former large β grains during cooling.

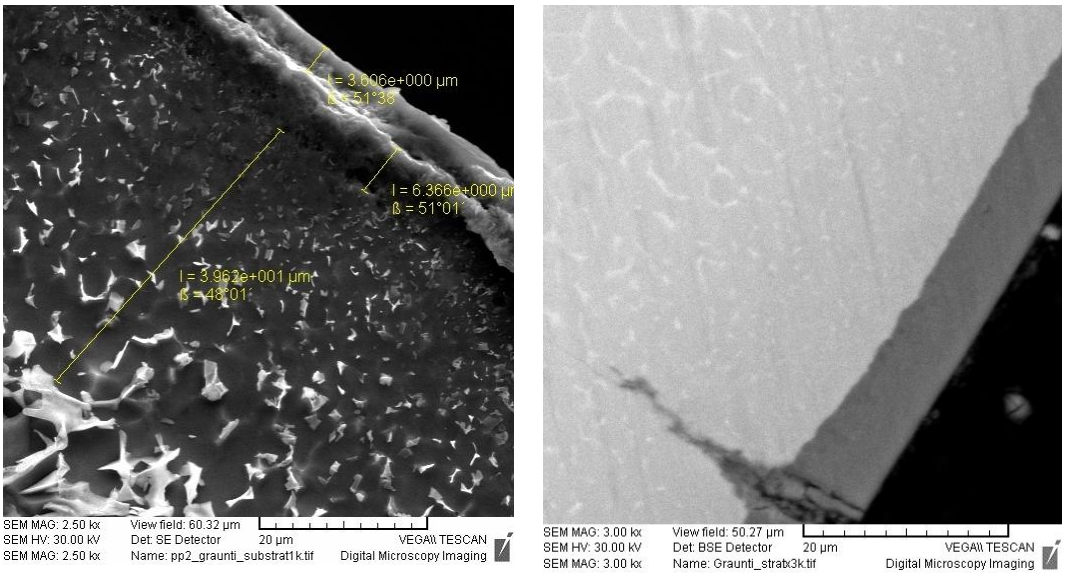

a) P2 sample **a) P4** sample

Fig. 5. a) Secondary electron image and **(b)** back-scattered image of alloy and oxide microstructures (samples **P2** respectively **P4**).

In Figure 5, are presented the following: (a) - a secondary electron (SE) image after etching for P2 sample and (b) - a BSE image of P4 sample, without chemical etching. The SE image of P2 confirms double-layered oxide. The oxide thickness of P4 is 6 μm, and in P2 sample is double, 10μm.

In the SE image (Figure 5.a), three layers with microstructures distinguishing from basis alloy (beta-zirconium phase) are presented. BSE image (Figure 5.b) distinguishes two layer differentiated by atomic contrast, dark-grey for oxide (it does not matter how many layers), light grey for alloy, and the grain boundaries of zirconium alloy, enriched in niobium, are highlighted in white. Therefore, the layer with small equiaxed grains (~40 μm in P2 sample) is obviously a layer composed from alpha zirconium grains stabilised by oxide layer or generated by the oxygen diffused in the alloy during heating period. The oxide are formed at 700^{o}C and, by heating the sample up to 1000^{o}C, a part of oxygen from layer diffuses in the alloy because of high oxygen solubility at the higher temperature.

All investigated samples present a similar layer.

In conclusion, under the oxide layers, the scanning electron microscopy revealed the existence of a layer consisting of alpha zirconium grains. The grain size in this layer decreases towards metal-oxide interface at values less than 0.1μm.

If the oxide crystallites replicate the alloy grain structure, the structure with α-Zr equi-axed grains is reproduced in oxide layer.

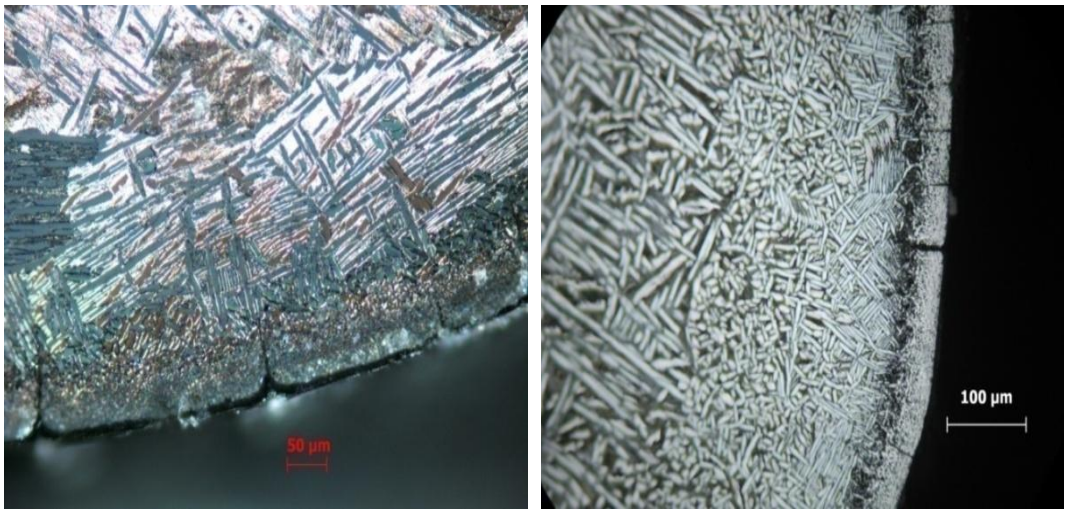

a) **b)**

Fig. 6. Metallographic images of alloy and oxide microstructure (**a) P1** and **b) P2** samples).

Light optical microscopy (Figure 6) has revealed that the oxide films are friable and heavily cracked. The oxide is in compression at the metal oxide interface, but it is relaxed toward the free surface by cracking.

Figure 6 presents a cross-section overall image of oxides and microstructures of P1 (a) and P2 (b) samples, after cooling from 1000 ^{o}C, obtained by metallographic methods. The cracks, initiated in oxide, passed by α–Zirconium layer and stopped in the next layer.

The figure 7a) presents a backscattered image of microstructure in sample P4. This image shows the grain boundaries from sample and also an oxide layer which consist in multiple layers. This microstructure was examined by energy dispersive X-ray spectrometer (EDS); the fluorescence spectrum was processed in the points marked on the picture.

An X-ray characteristic spectrum is also presented in figure 7b). In table 3 are presented the results of elemental composition in each point from picture 7a, the spectrum being processed by Quantax 400 software with an automatic standardless method (PB/ZAF standardless [3]).

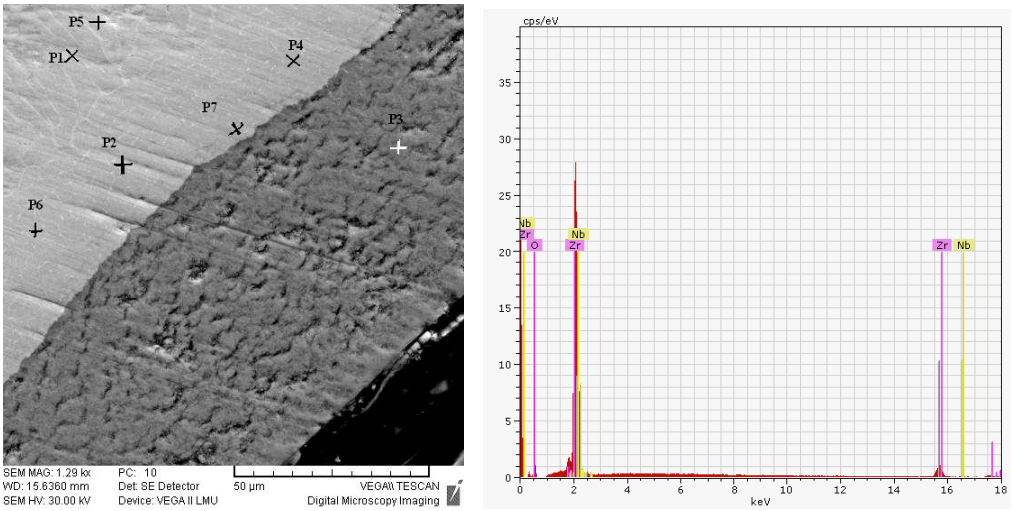

a) **b)**

Fig. 7. a) Backscattered electron image with atomic contrast; points where was determined the elemental composition by EDX; **b)** a X-Ray spectrum processed by Quantax 400 software.

Table 3. The elemental composition in the points from picture 7a.

No. sample	Zr content [% wt]	O content [% wt]	Nb content [% wt]
P_1	94	0	6
P_2	96.7	0	3.3
P_3	72.4	27.6	0
P_4	96.5	0	3.5
P_5	93.3	0	6.7
P_6	96.9	0	3.1
P_7	96.8	0	3.2

When the oxygen content in zirconium exceeds 26 percent by weight (wt%), the point P_3 from picture 7a), zirconium dioxide forms. This oxide, ZrO_2, is a brittle ceramic and it is considered to no offer effective resistance at fracture during thermal transients. At temperatures above 610^{o}C, the hexagonal close packed matrix of alloy, the α phase, starts to transform to a body centred cubic structure, the β phase. However, oxygen that diffuses into metal beneath the zirconium dioxide raises this transformation temperature. The layer immediately under oxide remains in alpha phase (points P_4, P_7, P_2, P_6) , and is called the stabilized alpha layer. This layer is also brittle and is generally considered to no offer resistance at fracture by thermal shock. Less oxygen diffuses into the central region of tube wall thickness, so that the transformation to the beta phase may be complete at temperature in a range of 950–1000 ^{o}C.

If the oxygen content of beta layer remains below certain limits, sufficient ductility is retained to offer resistance to fracture. Consequently, the β layer is the most important layer with respect pressure tube failures during loss of cooling accidents. In our tests, in the specific layer, with α grains which grew-up inside of former large β grains during cooling, the niobium content was 6%, and oxygen content was 0.

Conclusions

- The samples from Zr-2.5% wt Nb, oxidised at 700^{o}C, displays a layered structure:
  - Oxide layer;
  - A layer with alpha zirconium equi-axed grains;
  - A layer with Widmanstatten mixture of α/β plates;
  - A specific layer with β grains which grew-up inside of former large β grains during cooling.
- The grain size in alpha zirconium equi-axed grains layer decreases towards metal-oxide interface;
- The oxide films are friable and heavily cracked;
- The perpendicular cracks initiated in oxide passed by α–Zirconium layer and arrested in the next layer. Its propagate by weaker α–Zr equi-axed grain boundaries;
- Parallel cracks are present in thicker oxides producing a layered oxide;
- Oxidation stress relief promote fibre texture or columnar crystallites;
- The metal oxide interface undulates with increasing of oxide thickness.

R E F E R E N C E S

[1] Maria Mihalache, Tiberiu Meleg, V. Ionescu, *Micro structural changes in oxidized Zr 2.5%Nb alloy by thermal transients*, NUCLEAR 2009 International Conference, ISSN 2066-2955, 27-29 May 2009 Piteşti, România.

[2] *** - *TESCAN – Scanning Electron Microscope – Instruction for use*.

[3] Peter J. Goodhew, John Humpreys, Richard Beanland, *Electron Microscopy and Analysis*, 2001, Taylor and Francis, New York.